KSABC
The Korean Society for Applied Biological Chemistry

ARTICLE

Open Access

Check for updates

Murraya koenigii (L.) Sprengel seeds and pericarps in relation to their chemical profiles: new approach for multidrug resistant *Acinetobacter baumannii* ventilator-associated pneumonia

Riham A. El-Shiekh[1*] , Rana Elshimy[2,3], Asmaa A. Mandour[4], Hanaa A. H. Kassem[1], Amal E. Khaleel[1], Saleh Alseekh[5,6], Alisdair R. Fernie[5,6] and Mohamed A. Salem[7,8]

Abstract

Acinetobacter baumannii is without a doubt one of the most problematic bacteria causing hospital-acquired nosocomial infections in today's healthcare system. To solve the high prevalence of multi-drug resistant (MDR) in *A. baumannii*, we investigated one of the medicinal plants traditionally used as antibacterial agent; namely *Murraya koenigii* (L.) Sprengel. The total methanolic extracts of seeds and pericarps were prepared and their anti-bacterial activity was assessed using the agar diffusion method and minimum inhibitory concentration (MIC) was then calculated as compared to tigecycline. Then, an in-vivo murine model was established which confirmed the promising activity of *M. koenigii* seeds in demonstrating anti-bacterial and anti-inflammatory actions. The histopathological study of lungs, scoring of pulmonary lesions, counting of bacterial loads after infection by multi-drug resistant *A. baumannii* all provided evidence to support these findings. LC–MS/MS profiling coupled to molecular networking and chemometrics detected the presence of carbazole alkaloids, and coumarins as dominate metabolites of the active seed extracts. Positively correlated metabolites to antibacterial potential were 6-(2′,3′-dihydroxy-3-methylbutyl)-8-prenylumbelliferone, scopoline, and 5-methoxymurrayatin. An in-silico study was also performed on the crystal structure of MurF from *A. baumannii* (PDB ID: 4QF5), the studied structures of the mentioned extracts revealed good docking interaction at the active site suggestive of competition with the ATP ligand. These collective findings suggest that extracts of *Murraya koenigii* (L.) Sprengel seed is a novel prospective for the discovery of drug candidates against infections caused by MDR *A. baumannii*.

Keywords *Murraya koenigii* seeds and pericarps, MDR *A. baumannii*, LC/MS/MS, Chemometrics, Metabolomics, Molecular networking

---

*Correspondence:
Riham A. El-Shiekh
riham.adel@pharma.cu.edu.eg
Full list of author information is available at the end of the article

El-Shiekh *et al. Applied Biological Chemistry*   (2024) 67:35

Page 2 of 19

Introduction

Acinetobacter baumannii is a prominent and increasingly prevalent bacterium that causes severe illness and mortality [1]. It is one of the most common nosocomial diseases due to its capacity to develop mechanisms of resistance to many last-line antimicrobial treatments containing carbapenems [2–4]. In 2017, the World Health Organization (WHO) designated this bacteria as a priority-1 pathogen [5]. The bacteria lead to a wide range of infections, including ventilator-associated pneumonia, soft tissue, skin, wound, and urinary tract infections [6].

Most *A. baumannii* infections occur in seriously ill patients in the intensive care unit setting accounting for up to 20% of infections in ICUs worldwide [7]. Furthermore, the prevalence of *A. baumannii* infections in the community has been steadily growing. The multi-drug-resistant *A. baumannii* (MDRAB) phenotype may invade both biotic and abiotic surfaces and form as biofilm. Numerous anti-bacterial medications, such as tigecycline, carbapenem, polymyxin, and non-antibiotic therapy, are in demand due to *A. baumannii*'s pathogenicity [8]. The detection of lactamase, low permeability of the outer membrane (OM), and effective pump systems are the primary causes of MDRAB resistance to traditional antibacterial drugs [8].

Colistin and tigecycline are antibiotics of last resort used to treat a variety of multidrug-resistant bacteria, although there have been reports of antibiotic resistance against these drugs worldwide [9]. In perspectives of therapeutic strategies, herbal medicines are one of the probable approaches, which is an efficient alternative to develop several bioactive derivatives.

Curry (*Murraya koenigii* (L.) Sprengel) is a small aromatic shrub in the Rutaceae family [10]. Phytochemical study of its pericarps and seeds extracts revealed the existence of alkaloids, flavonoids, and phenolic contents, all of which have enormous potential to improve consumer health and reduce illness risks [11]. As such *Murraya* species can be considered as rich source of antibacterial compounds including carbazole alkaloids, and phenolics [12–14].

It is known that MurF is essential during peptidoglycan biosynthesis. It is an appealing target for multiple resistant bacterial treatment [15]. Discovery of novel therapeutic compounds is urgently needed to overcome bacterial resistance. Therefore, an in-silico approach using the C-Docker protocol in Discovery Studio 4.0 Software can be performed on the metabolites that are positively correlated with the antibacterial activity.

In continuation of our teams attempts to explore novel alternatives to last-resort therapies to avoid treatment failure against MDR infection [16–21], here we investigated *Murraya koenigii* (L.) Sprengel seeds and pericarps as anti-*A. baumannii*, where their chemical profiles were studied using LC/MS/MS. In silico studies and correlation analysis revealed that 6-(2′,3′-dihydroxy-3-methylbutyl)-8-prenylumbelliferone, scopoline, and 5-methoxymurrayatin as the most promising bioactive antibacterial metabolites.

Material and methods

Plant material

Seeds and pericarps of *Murraya koenigii* (L.) Spreng. (Family Rutaceae) were collected in September 2022 from Orman botanic garden (Giza, Egypt), authenticated by Mrs. Therese Labib, Botanical Specialist and Consultant at Orman and Qubba Botanical Gardens, Egypt. The voucher specimen was deposited in the herbarium of Cairo University's Pharmacognosy Department, Faculty of Pharmacy (#5.5.2022I).

Preparation of the extracts

Fresh pericarps (350 g) and 150 g of fresh seeds were air-dried and extracted by methanol (3×5 L) by maceration for 3 days. The collected extracts were filtered and evaporated under reduced pressure to give 28, and 13 g of total methanolic extract of *M. koenigii* pericarps and seeds, respectively.

Chemical profiling, molecular networking and metabolites annotation

Aliquots of the samples (2 mg) were re-suspended in 1000 μL methanol: water (UPLC-grade, 1:1, v/v) and moved to the autosampler, 2 μL was injected and separated on RP High Strength Silica (HSS)T3 C18 column (100 mm×2.1 mm having 1.7 μm diameter particles, Waters), using a Waters Acquity UPLC system. The mass spectra were obtained by full scan MS in positive ionization mode on an exact high resolution Orbitrap-type MS (Thermo-Fisher, Bremen, Germany) [22]. Metabolites were identified using their mass spectra, and by comparison with our in-house database and the references literature.

To obtain the online workflow, the mzXML files (Additional file 1: Table S1) were uploaded to the GNPS online platform [23, 24]. The constructed MN and its settings are available at https://gnps.ucsd.edu/ProteoSAFe/status.jsp?task=0e03844516104989b9d6a810ce3d96bc. For further processing and visualisation, network files were loaded into the open-source software platform Cytoscape 3.9.1 (https://cytoscape.org/download.html) [25].

Microorganisms

Extensively drug-resistant *A. baumannii* (XDRAB) strains clinical isolate (Additional file 1: Fig. S1) was collected from a tertiary care center in Cairo from a post

El-Shiekh *et al. Applied Biological Chemistry*   (2024) 67:35

Page 3 of 19

covid secondary bacterial infected patient and characterized in our previous work [26].

In vitro antibacterial assay
Preliminary screening of antibacterial activity was first screened for inhibitory zone by the agar disc-diffusion method according to CLSI guidelines as described before [27, 28]. Furthermore, the microbroth dilution method was implemented to determine MIC (the minimum bacteria growth inhibitory drug concentration) [29].

In vivo antibacterial assay
Male Balb C mice (22 to 25 g, 8 weeks) were obtained from the Egyptian Drug Authority, and kept in a standard controlled condition. The protocol was approved by the Animal Experiment Ethics Committee of the National Hepatology & Tropical Medicine Research Institute (NHTMRI) for Research Ethics Committee (REC) (#NHTMRI REC A5-2023). All C57BL/6 mice were anesthetized by inhaling isoflurane [30]. Then the mice were in the position of head up and upright, and *A. baumnii* suspension was dripped into the nasal cavity for 1×10^9 cfu in 50 μL of phosphate-buffered saline (PBS). The mice in Sham group were dripped with the same volume of normal saline by the same method. After inoculation, the mice kept their heads upright for 20 s to ensure that bacterial suspension or normal saline could enter both lungs evenly due to gravity. When the mice woke up, they were placed in the cage to eat freely. After an incubation period of 4 h, all the infected mice were randomly divided into five groups (n = 10) as follows:

(1) The Sham control group (without treatment).

(2) Untreated group.

(3 and 4) The plant groups (oral administration at 200 mg/kg every 24 h).

(5) The Tigecyclin treatment group (subcutaneous administration of Tigecyclin at 75,000 U/kg every 12 h).

The Sham and model group were administrated by oral gavage with the same volume of normal saline. After 72 h of drug administration, the animals were sacrificed by cervical dislocation, lungs were collected for biochemical and histopathological examinations [31].

Biochemical examination Interferon-gamma (IFN-γ) (CEK1476), tumor necrosis factor alpha (TNF-α) (CSB-E04741m), IL-6 (CSB-E04639m), IL10 (CSB-E04594m), IL12 (MBS2568055), and Myeloperoxidase (MPO) (MBS700747) were measured following the manufacturer's guides.

Histopathology and lesion score Hematoxylin and eosin (H&E) staining was performed [32], and examined by Leica DM4 B light microscope (Leica, Germany). Images were captured by Leica DMC 4500 digital camera (Leica, Germany). The severity of the detected lesions was evaluated as follow (−) = absent, (+) = mild, (++) = moderate and (+++) = severe (Qualitative scoring system).

Pulmonary bacterial loads Lungs were removed aseptically and homogenized with a tissue homogenizer in 5 ml of sterila saline. Homogenized lung samples are then serially diluted in sterile saline and plated on Lauria bertani agar plates (Additional file 1: Fig. S2) [33].

In silico study The crystal structure of MurF from *Acinetobacter baumannii* complexed with ATP was successfully downloaded from Protein Data Bank (PDB ID: 4QF5) [15]. The protein was cleaned. Also, hydrogen atoms was added to complete any missing residues in amino acids. It's worth noting that water molecules was removed and all unneeded molecules. Force Field CHARMm and MMFF94 partial charge was successfully applied. Protein was prepared and minimized; the active site was well defined as ATP is the main ligand. The ligand ATP was removed before docking of the tested compounds.

Statistical analysis Analysis of Variance (ANOVA) was used to establish statistical significance. The aligned peak list obtained by MZmine software and was exported as a CSV file, with information about retention time, the feature ID number, peak intensity, and mass-to-charge ratio (*m/z*). All variables were $\log_{10}$-transformed scaled to Pareto variance before PCA and OPLS-DA. The web-based platform Metaboanalyst 5.0 (https://www.metaboanalyst.ca/) was utilized for Multivariate data analysis [34].

Results
Chemical profiling
The methanolic extracts of the *M. koenigii* seeds (MKS) and pericarps (MKF) were analyzed using UPLC-MS/MS (Table 1), where the mass spectra in positive modes resulted in the identification of 102 compounds viz. 40 alkaloids, 35 phenolics (11 flavonoids, five phenolic acids, and 19 coumarins), five organic acids, five phospholipids, three fatty acids, ten amino acids, one quinoline derivative, one sugar, one vitamin, and one fatty amide. The mass fragmentation of those compounds was compared to reference papers as cited in Table 1.

The most prominent compounds belong to the carbazole alkaloids class; mukoline, koenimbine, murrayanine, and murrastanine A (peaks # **72**, # **76**, # **101**, and # **102**) in seeds where, koenimbine, isomahanine, 9-formyl-3-methyl carbazole, and koenine (peaks # **65, 76**, # **73**, # **85**, and # **54**) with Mexoticin (# **94**) as coumarin were the prominent in pericarps. In the supplemental materials shown in Additional file 1: Figs. S3–S6, the representative MS/MS spectra of selected compounds among the major classes are shown.

El-Shiekh *et al. Applied Biological Chemistry*   (2024) 67:35

Page 4 of 19

Table 1 UPLC/MS/MS chemical profiling of *M. koenigii* seeds (MKS) and pericarps (MKP) total methanolic extracts analyzed in positive ionization mode

Compound No.	m/z	RT (min)	Compound name	Molecular formula	MKS	MKP	Main fragments	Chemical class	References
1	175.11622	0.57	Arginine	$C_6H_{14}N_4O_2$	7,642,201.43	977,949.1231	157, 142	a. a	PubChem
2	104.10738	0.61	Choline	$C_5H_{14}NO$	76,350,000	24,250,000	104	a. a	Mass bank
3	116.07087	0.69	L-Proline	$C_5H_9NO_2$	210,000,000	134,000,000	116	a. a	Mass bank
4	365.10538*	0.70	Sucrose	$C_{12}H_{22}O_{11}$	184,000,000	51,200,000	103, 147, 217, 129.0	s	PubChem
5	130.08636	0.69	*N*-Methyl proline	$C_6H_{11}NO_2$	1,170,000,000	741,000,000	130	a. a	PubChem
6	130.09767	1.09	Pipecolic acid	$C_6H_{11}NO_2$	301,569.2959	0	130	a. a	PubChem
7	152.10814	1.74	Methyltyramine	$C_9H_{13}NO$	58,658.0631	63,021.9247	152	a. a	PubChem
8	182.08133	1.81	Tyrosine	$C_9H_{11}NO_3$	80,303,487.6	2,655,587.393	165	a. a	Mass bank
9	166.08631	3.17	L-Phenylalanine	$C_9H_{11}NO_2$	13,500,000	2,944,520.029	166	a. a	Mass bank
10	181.04932	4.22	*trans*-Caffeic acid	$C_9H_8O_4$	2,399,231.1	2,287,464.008	137, 145, 161	ph. a	[53]
11	175.03883*	5.34	Vanillin	$C_8H_8O_3$	6085.8	35,193.795	151	or. a	Mass bank
12	310.16471	5.62	Sinapine	$C_{16}H_{24}NO_5$	27,450,000	618,316.7549	311, 251, 207, 154, 134, 175, 147	al	[54]
13	195.06488	6.14	Ferulic acid	$C_{10}H_{10}O_4$	543,150.3	406,270.7775	116, 134, 151, 179, 163	ph. a	[53]
14	207.06514	6.160	Sinapic acid	$C_{11}H_{12}O_5$	0	274,217.6905	181, 133	ph. a	[55]
15	177.05462	6.37	Ferulic acid	$C_{10}H_{10}O_4$	487,415.2455	1,315,427.147	151	ph. a	[53]
16	481.26193	6.44	Myricetin-*O*-galactoside	$C_{21}H_{20}O_{13}$	3,668,754.278	6,818,027.776	317, 272, 181, 152	fl	[56]
17	611.15961	6.47	Quercetin-*O*-robinobioside	$C_{27}H_{30}O_{16}$	0	6283.2525	303, 257, 229, 153	fl	[53]
18	435.0918	6.48	Quercetin-*O*-pentoside	$C_{20}H_{18}O_{11}$	5413.8	306,761.175	303, 257, 153	fl	[53]
19	597.14489	6.50	Quercetin-3-O-arabinoglucoside	$C_{26}H_{28}O_{16}$	0	830,138.1678	303, 257, 153	fl	[53]
20	449.10703	6.97	Quercitrin	$C_{21}H_{20}O_{11}$	54,517.05	44,918.4225	303, 257, 153	fl	[53]
21	465.10283	7.04	Isoquercetrin	$C_{21}H_{20}O_{12}$	0	2,656,850.99	303, 257, 153	fl	[53]
22	303.0497	7.04	Quercetin	$C_{15}H_{10}O_7$	0	2,656,850.99	153, 137	fl	[57]
23	172.03785	7.33	3-Cyanocoumarin	$C_{10}H_5NO_2$	276,376.2057	160,704.7273	143, 127	c	Pub Chem
24	609.14496	7.37	Quercetin 3-[6″-(3-hydroxy-3-methylglutaryl)galactoside]	$C_{27}H_{28}O_{16}$	0	1,884,947.526	303	Fl	[58]
25	173.08553	7.52	1,4-Cyclohexanedicarboxylic acid	$C_8H_{12}O_4$	4,673,649.844	7,212,019.694	173, 109	or. a	Pub Chem
26	163.13280	7.66	Caffeic acid	$C_9H_8O_4$	9,272,176.45	9,700,346.324	145, 135, 119, 108	Ph.a	[59]
27	146.06339	9.48	6-Quinolinol	C_9H_7NO	9,550,000	2,684,161.91	146	q. d	-
28	275.20038	10.79	Toddalenone	$C_{15}H_{14}O_5$	0	246,958.313	259, 243, 231, 216, 188, 173, 160, 145	c	[60]
29	293.21073	10.79	8-[3-oxo-2-[(E)-pent-2-enyl]cyclopenten-1-yl]octanoic acid	$C_{18}H_{28}O_3$	117,714.6141	210,026.6953	279, 189	or. a	-
30	389.12283	10.82	5-Demethylnobiletin	$C_{20}H_{20}O_8$	11,469.15	1,957,974.795	359, 341, 328, 285, 215	fl	[61, 62]
31	279.15697	10.99	Meranzin hydrate	$C_{15}H_{18}O_5$	0	5,879,825.79	260, 220, 219, 218, 217, 202, 190, 189	c	[63]
32	295.22659	11.45	9-hydroxy-10,12-octadecadienoic acid	$C_{18}H_{32}O_3$	900,991.0101	0	231, 155, 143	f. a	-
33	373.1282	11.62	Isosinensetin	$C_{20}H_{20}O_7$	0	9740.5875	358, 343, 329, 297	meth. fl	[62]
34	293.21073	10.79	8-[3-oxo-2-[(E)-pent-2-enyl]cyclopenten-1-yl]octanoic acid	$C_{18}H_{28}O_3$	117,714.6141	210,026.6953	279, 189	or. a	-

El-Shiekh *et al. Applied Biological Chemistry*   (2024) 67:35

Page 5 of 19

Table 1 (continued)

Compound No.	*m/z*	RT (min)	Compound name	Molecular formula	MKS	MKP	Main fragments	Chemical class	References
35	345.224624	12.149	Murralonginol isovalerate	$C_{20}H_{24}O_5$	6,652,025.661	6,822,046.414	231 227 199 189 149 131, 115	c	[64]
36	287.26916*	12.20	Mukoenine A/ Girinimbilol	$C_{18}H_{19}NO$	3,867,078.249	3,902,050.4	265, 209	al. car	[65]
37	373.12836	12.30	Sinensetin	$C_{20}H_{20}O_7$	32,761.05	15,288.6825	358, 343, 329, 297	meth. fl	[62]
38	389.25073	12.35	Panitin D	$C_{21}H_{24}O_7$	9,663,560.23	9,981,945.935	359, 289	c	[66]
39	353.22980	12.35	Norrangiformic acid	$C_{20}H_{36}O_6$	9,663,560.23	9,981,945.935	219, 189, 131	or. a	-
40	345.27464	12.37	Isomurralonginol isovalerate	$C_{20}H_{24}O_5$	0	21,750,000	231 227 199 189 149 131, 115	c	[64]
41	274.27389	12.44	Lauryldiethanolamine, 2-[dodecyl(2-hydroxyethyl) amino]ethanol	$C_{16}H_{35}NO_2$	12,100,000	12,850,000	227, 189, 131	ph. l	-
42	318.30011	12.50	Phytosphingosine	$C_{18}H_{39}NO_3$	623,500,000	645,000,000	281, 189, 131	ph. l	-
43	291.19478	12.51	5,7-dimethoxy-8-(3-methyl-2-keto-butyl) coumarin	$C_{16}H_{18}O_5$	5,885,914.12	5,888,624.311	217, 163	c	[67]
44	240.23209	12.52	1-Formyl –3 methoxy-6-methyl carbazole	$C_{15}H_{13}NO_2$	928,179.825	1,067,860.417	209, 189	al. car	[68]
45	242.08104	12.62	Mukoeic acid	$C_{14}H_{11}NO_3$	22,250,000	23,450,000	227, 213, 199, 196, 153	al. car	[69]
46	333.26335	12.79	6-(2',3'-dihydroxy-3-methylbutyl)-8-prenylum-belliferone	$C_{19}H_{24}O_5$	453,491.6069	4,248,155.097	314, 299, 281, 241, 227, 213	c	[70]
47	355.24535	12.80	Scopolin	$C_{16}H_{18}O_9$	3,536,652.666	0	311, 193, 163	c	[71]
48	256.29973	12.92	Mukonine	$C_{15}H_{13}NO_3$	5,802,146.81	0	237, 207, 189	al. car	[72]
49	563.34019	13.01	Toddalosin	$C_{32}H_{34}O_9$	95,265.02805	76,083.57335	281, 189	di. c	[73]
50	393.30866	13.29	5-Methoxymurrayatin	$C_{21}H_{28}O_7$	0	5,024,939.153	291, 275, 249, 219, 161	c	[74]
51	241.17753	13.32	10-Methoxy-7-methyl-2H-benzo[g]chromen-2-one	$C_{15}H_{12}O_3$	16,550,000	8,828,620.29	235, 213, 211, 147, 145	c	[75]
52	264.10180	13.38	Isogirinimbine	$C_{18}H_{17}NO$	11,031,096.4	15,400,000	249, 236, 220	al. car	[53]
53	329.22976	13.44	7-Geranyloxy-6-methoxy-coumarin	$C_{20}H_{24}O_4$	40,400,000	44,950,000	192, 177, 164, 149	c	[75]
54	280.13330	13.45	Koenine	$C_{18}H_{17}NO_2$	37,600,000	68,600,000	279, 264, 251, 248	al. car	[53]
55	310.23512	13.46	Iso-Koenigine	$C_{19}H_{19}NO_3$	27,350,000	19,850,000	294, 278, 263, 227	al. car	[76]
56	288.25318	13.46	Lauryl diethanolamide, N,N-bis(2-hydroxyethyl) dodecanamide	$C_{16}H_{33}NO_3$	47,900,000	46,550,000	275, 253	ph. l	-
57	343.20905*	13.49	Murrayanone	$C_{17}H_{20}O_6$	54,000,000	50,450,000	321, 250, 249, 235, 234, 206, 204, 163, 121	c	[77]
58	431.26214	13.53	Tocopherol	$C_{29}H_{50}O_2$	25,750,000	22,300,000	431, 165	v	-
59	549.36085*	13.53	Murrafoline C	$C_{36}H_{34}N_2O_2$	13,350,000	14,600,000	511, 469, 263, 256, 248, 227	al. car	[78]
60	341.161334*	13.62	Murrangatin acetate	$C_{17}H_{18}O_6$	5,977,754.904	6,277,441.261	261, 243	c	[79]
61	475.25943	13.69	Murrafoline B	$C_{32}H_{30}N_2O_2$	8,106,287.259	16,750,000	419, 278, 263, 248, 237, 211	al. car	[78]
62	258.20635	13.70	6, 7-Dimethoxy- 1-hydroxy-3-methyl-carbazole	$C_{15}H_{15}NO_3$	10,850,000	11,400,000	243, 238, 208, 204, 189	al. car	[80]
63	277.21608	13.85	FA 18:3 + 1O	$C_{18}H_{30}O_3$	0	4,471,821.225	255, 144	f. a	-
64	310.14389	13.87	Koenigine	$C_{19}H_{19}NO_3$	0	251,000,000	294, 278, 263, 227	al. car	[76]
65	294.11228	13.88	Koenimbine	$C_{19}H_{19}NO_2$	703,757.8632	14,000,000	279, 264, 251, 248	al. car	[53]
66	259.19031	13.91	Murrayone/ murralongin	$C_{15}H_{14}O_4$	5,401,031.872	6,206,718.388	259, 147, 131	c	[81]

Table 1 (continued)

Compound No.	*m/z*	RT (min)	Compound name	Molecular formula	MKS	MKP	Main fragments	Chemical class	References
67	332.33099	13.92	Mahanimbidine	$C_{23}H_{25}NO$	12,150,000	9,753,928.303	316, 289, 263, 249, 205	al. car	[82]
68	243.13551	14.07	Dehydroosthol	$C_{15}H_{14}O_3$	6,686,703.306	5,400,000	228, 212, 187, 183, 155, 131, 115	c	[83]
69	323.15146	14.22	Koenidine/ Koenigicine	$C_{20}H_{21}NO_3$	58,450,000	441,500,000	323.3, 308, 282	al. car	[84]
70	279.23165	14.23	Linolenic acid	$C_{18}H_{30}O_2$	8,446,326.588	5,211,895.507	255, 143	f. a	-
71	430.38909	14.28	Sorbitane Monostearate	$C_{24}H_{46}O_6$	2,905,584.903	5,112,299.484	279, 210	ph. l	-
72	249.18525	14.33	Mukoline	$C_{14}H_{13}NO_2$	1,764,592.179	0	212, 210, 198, 183, 167, 154	al. car	[85]
73	347.18725	14.49	Isomahanine	$C_{23}H_{25}NO_2$	58,000,000	0	292, 266, 251, 238, 226	al. car	[53]
74	421.23251	14.52	Bismurrayafoline A	$C_{28}H_{24}N_2O_2$	0	14,700,000	211, 181	al. car	[86]
75	278.11742	14.57	Murrastinine C/ murrayacine	$C_{18}H_{15}NO_2$	196,500,000	237,500,000	262, 235	al. car	[87, 88]
76	294.14796	14.57	Koenimbine	$C_{19}H_{19}NO_2$	995,500,000	1,590,000,000	279, 264, 251, 248	al. car	[53]
77	346.18011	14.67	Murrayacinine/ Murrastinine A	$C_{23}H_{23}NO_2$	0	83,550,000	345, 263	al. car	[89]
78	362.18479	14.86	Murrayamine B	$C_{24}H_{27}NO_2$	5,489,804.386	4,573,318.02	292, 266, 251, 238, 226	al. car	[53]
79	639.40742*	14.91	8, 8''- bis koenigine	$C_{38}H_{36}N_2O_6$	7,068,983.514	3,038,558.311	601, 585, 561, 308	al. car	[76]
80	595.38133	14.92	Murrafoline A	$C_{41}H_{42}N_2O_2$	8,726,698.764	5,107,492.778	579, 538, 511	al. car	[90]
81	280.91531	14.98	Murrayamine A	$C_{18}H_{17}NO_2$	32,400,000	15,400,000	263,235	al. car	[91]
82	264.10175	14.98	Girinimbine	$C_{18}H_{17}NO$	0	44,400,000	249, 236, 220	al. car	[53]
83	693.36661	14.99	Bis-pyrayafoline	$C_{46}H_{48}N_2O_4$	4,475,024.414	22,750,000	609, 347, 263	al. car	[92]
84	334.21672	15.0	Mahanimbilol	$C_{23}H_{27}NO$	3,960,307.007	9,418,516.407	264, 250, 249, 248, 210, 209, 180	al. car	[93]
85	210.09132	15.10	9-Formyl-3-methyl carbazole	$C_{14}H_{11}NO$	832,925.0605	4,664,774.08	209, 183, 181	al. car	[94]
86	280.26337	15.12	Murrastinine B	$C_{18}H_{17}NO_2$	22,250,000	4,938,563.829	264, 251, 248	al. car	[87]
87	363.31023	15.25	3,6,9,12-Tetraoxatetracosan-1-ol	$C_{20}H_{42}O_5$	18,800,000	20,100,000	270, 227	ph. l	-
88	280.91531	15.28	Pyrayafoline B/ Koenine	$C_{18}H_{17}NO_2$	37,500,000	51,000,000	279, 264, 251, 248	al. car	[53]
89	585.23724	15.37	8,8'-Bismurrayamine A, dimethyl ether	$C_{38}H_{36}N_2O_4$	0	14,000,000	571, 555, 527	al. car	Pub Chem
90	256.26334	15.49	Mukonine isomer	$C_{15}H_{13}NO_3$	37,500,000	20,700,000	237, 207, 189	al. car	[72]
91	361.20343	15.57	Paniculatin	$C_{20}H_{24}O_6$	18,050,000	89,550,000	289, 232, 205, 175, 149, 145	c	[95]
92	282.27899	15.62	Oleamide	$C_{18}H_{35}NO$	163,000,000	26,200,000	255	f. am	-
93	108.08112	15.67	N-Methylaniline	C_7H_9N	246,500,000	105,500,000	108	a. a	
94	309.13238	16.1	Mexoticin	$C_{16}H_{20}O_6$	0	14,800,000	292, 266, 251, 238, 226	c	[53]
95	633.14994*	16.35	Rutin	$C_{27}H_{30}O_{16}$	109,600,000	78,350,000	465, 303	fl	[96]
96	249.14614	16.60	Koenoline	C14H13NO2	876,148.0045	1,194,907.637	227, 212, 210, 198, 183, 167, 154, 139 127	al. car	[97]
97	226.95136	17.0	Mukolinidine	$C_{14}H_{11}NO_2$	92,400,000	101,400,000	211, 183, 155, 139, 129, 127	al. car	[98]
98	362.92611	17.1	Murrayamine C	$C_{24}H_{27}NO_2$	11,800,000	11,800,000	292, 266, 251, 238, 226	al. car	[53]
99	196.01674	17.12	3-Formylcarbazole	$C_{13}H_9NO$	43,250,000	65,950,000	179, 154	al. car	[99]
100	282.91017	17.13	Euchrestine A	$C_{18}H_{19}NO_2$	37,200,000	52,350,000	225	al. car	[100]
101	226.01193	17.14	Murrayanine	$C_{14}H_{11}NO_2$	110,900,000	123,500,000	211, 183, 155, 139, 129, 127	al. car	[98]

El-Shiekh *et al. Applied Biological Chemistry*   (2024) 67:35

Page 7 of 19

Table 1 (continued)

Compound No.	m/z	RT (min)	Compound name	Molecular formula	MKS	MKP	Main fragments	Chemical class	References
102	214.00356	17.60	Murrastanine A	$C_{13}H_{11}NO_2$	4,480,991.944	5,036,686.238	199	al. car	[101]

* Adduct as [M + Na]$^+$

a.a.: amino acid, f. a.: fatty acid, al. car.: carbazole alkaloids, f. am.: fatty amide, fl.: flavonoids, ph. a.: phenolic acid, or. a.: organic acid, c. coumarins, di. c. Di coumarins, s.: sugar, ph. l.: phospholipids, met. Fl.: methylated flavonoids.MKS: *Murraya koenigii* seeds, MKP: *Murraya koenigii* pericarps

The numbers represent the peak area

The molecular networking approach was applied, and this enabled the direct visual examination of MS/MS data, as well as the observation of metabolite distribution among the various extracts (Fig. 1). It categorized molecules into families or clusters based on the similarity of their MS/MS fragmentation patterns.

### In vitro anti-*A. baumannii* study

Upon performing antibacterial susceptibility by Kirby's Bauer disc diffusion, *M. koenigii* seed extracts showed high antibacterial activity (21 mm) and could diminish bacterial growth with *A. baumannii* being sensitive towards the sample as well as tigecycline (20 mm). By contrast, *M. koenigii* fruit extracts were ineffective with inhibition zones of 10 mm (Table 2 and Additional file 1: Fig. S7). Furthermore, MICs for *M. koenigii* seeds

Table 2 Screening of antibacterial activity of *Murraya koenigii* seeds and pericarps against *A. baumannii*

Sample	Zone of inhibition in mm (Mean ± SD)	Interpretation	MIC (µg /mL)
DMSO	0.0 ± 0.0	R	–
Amikacin	0.0 ± 0.0	R	–
Tigecycline	20.0 ± 1.00	S	1
M. koenigii seeds	21.0 ± 1.00	S	32
M. koenigii pericarps	10.0 ± 1.00	R	125

R resistant, *S* sensitive

and fruit extracts were 32, and 125 ug/ml, respectively (Table 2).
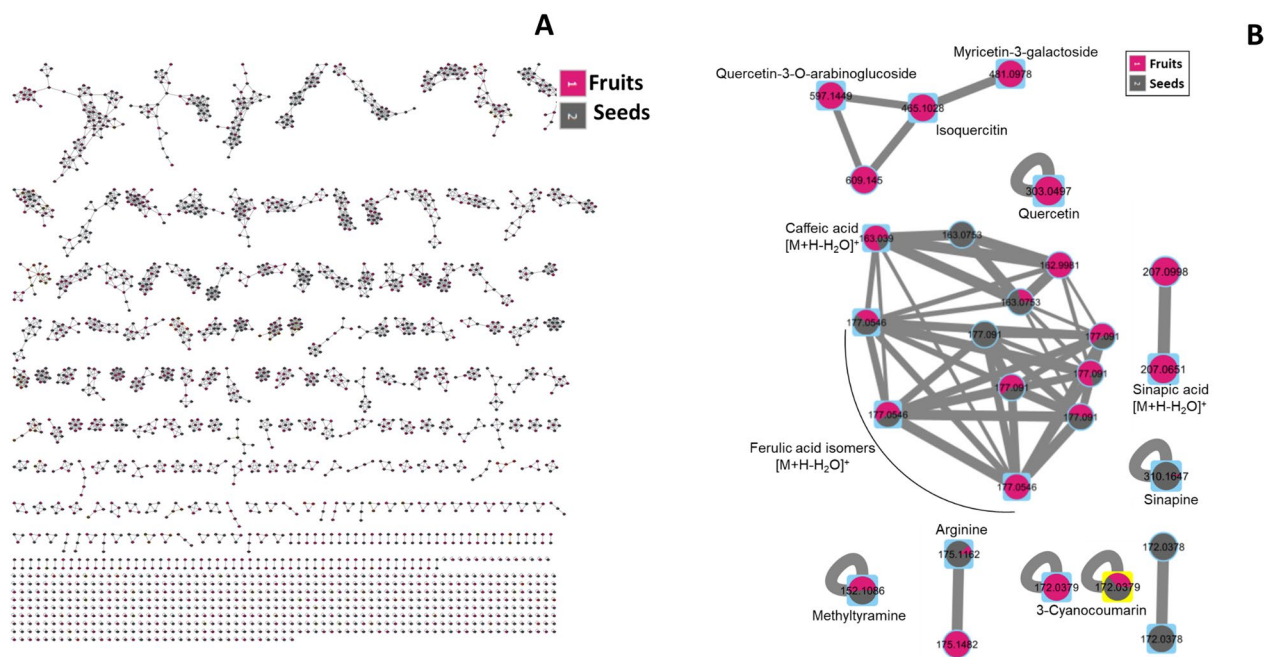
Fig. 1 **A** Molecular networking established using LC–MS/MS data in the positive ESI mode. **B** Selected nodes and clusters have been zoomed in. Single nodes are used to represent molecules that do not form groups. Nodes were also colored by organ type (seeds and pericarps) and labelled with their precursor m/z values. The nodes were also represented as a pie chart to show the semi-relative abundance of the identified molecule ions, with the borders indicating the mass differences between the connected nodes

El-Shiekh *et al. Applied Biological Chemistry*   (2024) 67:35

Page 8 of 19

In vivo anti-*A. baumannii* study

Hematological biomarkers

M. koenigii seed extracts and tigecycline envoked few changes in regard to these parameters. By contrast, the fruit extract showed higher levels of hematological biomarkers revealing higher inflammation and lower antibacterial activity (Fig. 2).

Histopathology

As illustrated in Fig. 3 and Table 3, no histopathological changes were observed in lung sections from normal group as normal bronchioles and alveoli were observed. By contrast, the untreated group exhibited severe diffuse pneumonia manifested by heavy inflammatory cells infiltrations that masked lung tissue with discreet area of pulmonary necrosis. The alveolar lumens were heavily infiltrated by inflammatory cells with presence of bacterial colonies. Blood vessels with severely congested. *M. koenigii* seeds extract treated mice showed marked improvement as most of the studied sections demonstrated mild interstitial mononuclear inflammatory cells infiltrations with clear alveolar lumen and mild vascular congestion. The *M. koenigii* pericarps extract treated group exhibited mild improvement as the examined tissue samples showed moderate inflammatory cells infiltrations in the interstitial tissue as well as multifocal areas of pneumonia. Tigecycline S/C group showed marked improvement as most of the examined sections were apparently normal, only a few sections exhibited mild interstitial infiltration with mononuclear inflammatory cells.

Pulmonary bacterial loads

M. koenigii seeds showed better anti *A. baumannii* than pericarps which had a moderate activity as revealed from bacterial loads results (Table 4).

Multivariate data analysis

Untargeted metabolomic analyses usually generate a complex dataset in terms of features and their corresponding intensities, thus, various dimensionality reduction methods including principal component analysis (PCA) and hierarchical cluster analysis (HCA) are performed to ease the process of visualizing the data. PCA
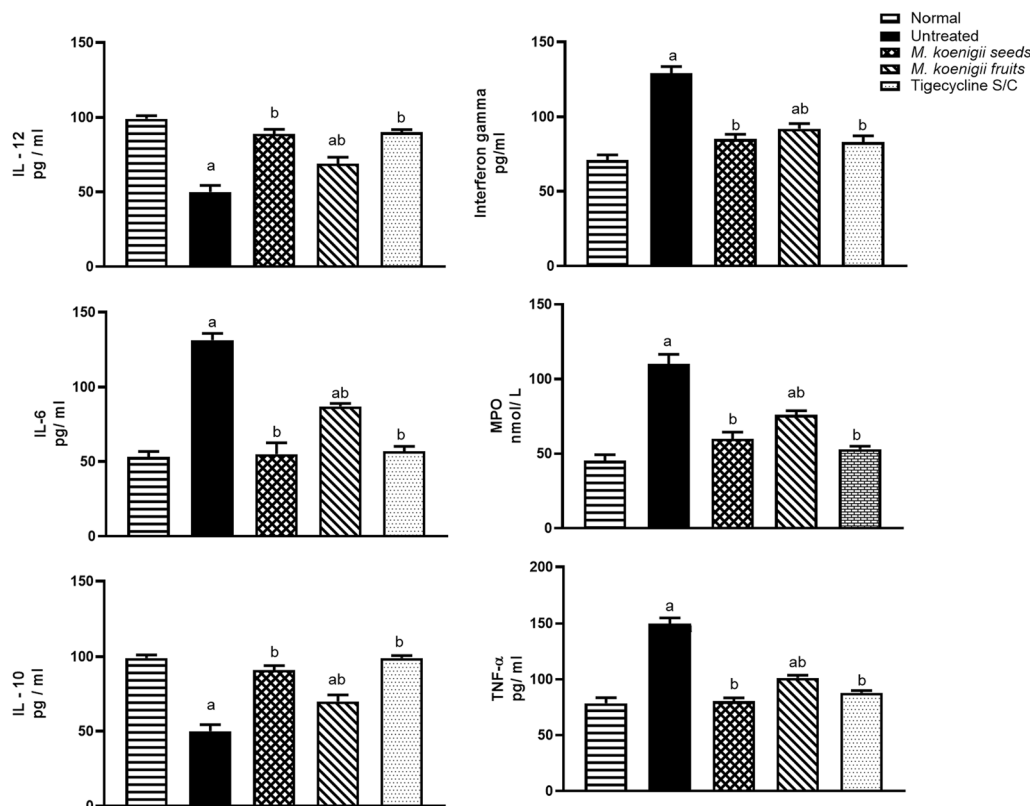
Fig. 2 Hematological biomarkers of seeds and pericarps of *M. koenigii* as compared to Tigecycline in *Acinetobacter baumannii* murine animal model. Data are expressed as mean ± SD. Statistical analysis was carried out by one-way ANOVA followed by Tukey's multiple comparison test. [a]Significant difference from normal group at $p < 0.05$. [b]Significant difference from infected group at $p < 0.05$. [ab]Significant difference from normal group and infected group at $p < 0.05$
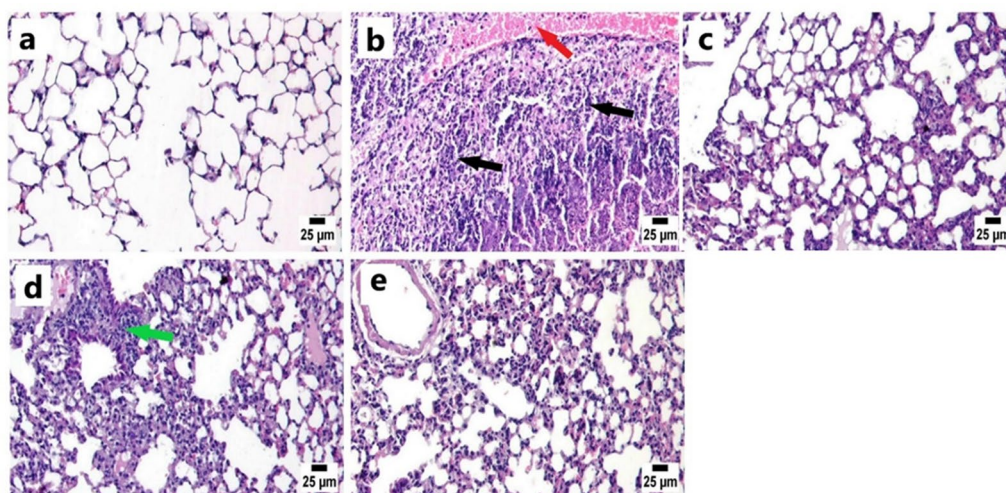
Fig. 3 Photomicrographs of lung by hematoxylin and eosin stain (H&E) showing normal structure of lung in normal group (**a**), intense inflammatory cells infiltration (black arrow) and severe congestion (red arrow) in untreated group (**b**), mild interstitial pneumonia in *M. koenigii* seeds treated group (**c**), moderate thickening of interalveolar wall with mononuclear inflammatory cells (green arrow) in *M. koenigii* pericarps treated group (**d**), mild interstitial pneumonia in Tigecycline S/C group (**e**)

Table 3 Qulitive lesion score of the detected histopathological alterations in lungs of different experimental groups

	Normal	Untreated	*M. koenigii* seeds treated group	*M. koenigii* pericarps treated group	Tigecycline S/C group
Inflammatory cells infiltration	−	+++	+	++	+
Pulmonary necrosis	−	+++	+	++	−
Vascular congestion	−	+++	+	+	+

(−) = absent, (+) = mild, (++) = moderate, (+++) = severe

**Table 4** Pulmonary bacterial loads against *A. baumannii*

	Groups				
	Sham	Model	M. koenigii seeds	M. koenigii pericarps	Tigecycline (S/C)
A. baumnii (CFU/g Lung)	Zero	Death	5×10^3	4×10^5	1.5×10^2

results are shown in Fig. 4A. As can be shown, PC1 and PC2 (87.1% and 10.1% of the total variance, respectively) well explained the variation of the samples (n = 3) as analyzed by LC/MS analysis. HCA are presented in Fig. 4B. These separated the samples into two clusters, revealing different chromatographic patterns of both organs.

The results of unsupervised analysis was further verified using the supervised orthogonal partial least squares discriminant analysis (OPLS-DA), Offering valuable insights into the distinguishing metabolites between the tested samples. The OPLS-DA score plot (Fig. 5A) explained 65.9% of the total variance and 15.3 of the orthogonal total variances, where seeds and pericarps segregated into two different nonoverlapping clusters. The loadings S-plot (Fig. 5B) was used to compare variable magnitude vs reliability, with axes displayed from the predictive component being the covariance P [1] versus the correlation P(cor) [1]. Isogirinimbine, scopoline, sinapine, isomahanine, mukoline, Murrastinine B, 8, 8″-bis koenigine, N-Methylaniline, sinensetin, and 5-Methoxymurrayatin were the discriminating metabolites of seeds. Furthermore, quercetin, isoquercitrin, toddalenone, bismurrayafoline A, norrangiformic acid, meranzin hydrate, 8,8'-Bismurrayamine A, dimethyl ether, Murrastinine C/ murrayacine, koenigine, and mexoticin were the discriminating metabolites in pericarps.

Pearson's correlation coefficients (r) were next used to determine the correlation between the abundance of the annotated metabolites in *M. koenigii* seed and fruit extracts and antibacterial activity, with Pearson's correlation coefficient (r) was ≥ 0.9 at p < 0.05. The compounds that discriminated fruit extract were 6-(2′,3′-dihydroxy-3-methylbutyl)-8-prenylumbelliferone,
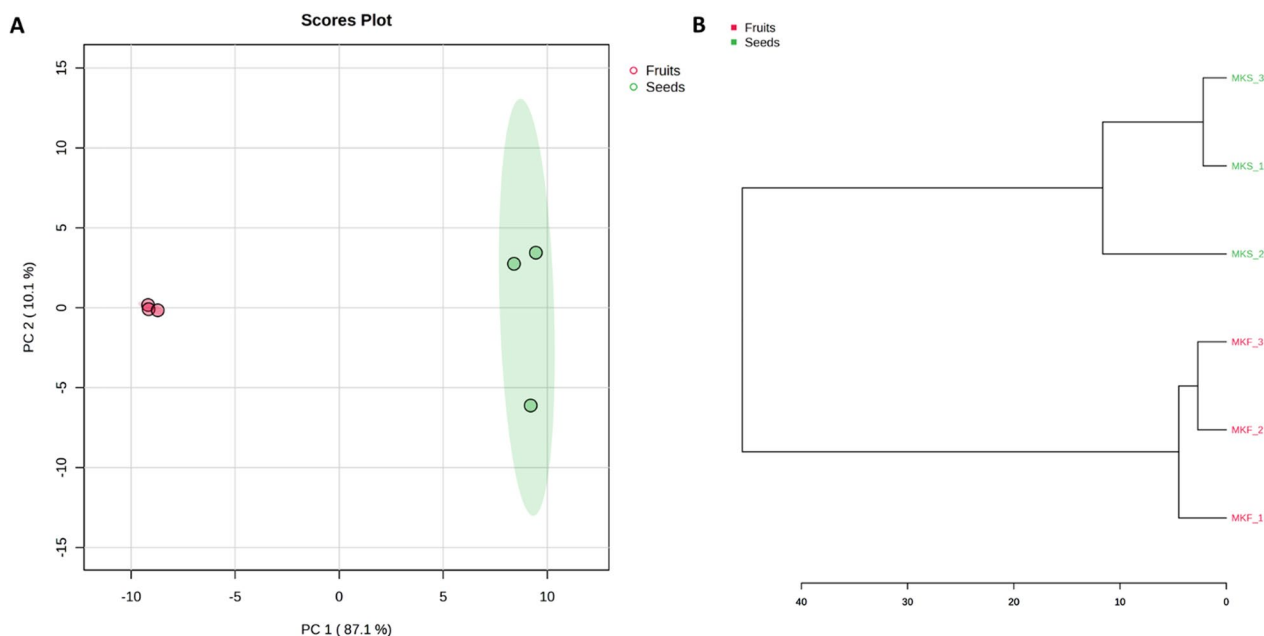
Fig. 4 **A** PCA and **B** HCA loadings plot. Multivariate data analysis was performed with the complete LC–MS dataset

scopoline, 5-demethylnobiletin, quercetin-O-pentoside, vanillin, mexoticin, koenigine, murrastinine C/ murrayacine, 8,8'-Bismurrayamine A, dimethyl ether, meranzin hydrate, norrangiformic acid, bismurrayafoline A, mukoeic acid, koenidine/ koenigicine, toddalenone, quercetin, quercetin-3-*O*-arabinoglucoside, and paniculatin. While the compounds discriminating theseed extract were tyrosine, isogirinimbine, isoquercetrin, 9-hydroxy-10,12-octadecadienoic acid, sucrose, koenimbine, and sinapine (Fig. 5C).

In addition, the metabolites that distinguished between active and inactive extracts were further validated by computing the VIP scores obtained from the OPLS-DA modelling of the active seed extract against the inactive fruit extract. As can be concluded, the discriminating metabolites were relevant to explain the variance when also having VIP scores > 1at $p < 0.05$ (Fig. 5C). The metabolites positively correlated to the antibacterial activity are shown in Table 5.

In silico study

The tested ligands were prepared, then docked into the binding site of MurF (*A. baumannii*). The binding mode of the tested compounds was analyzed and compared to that of the ligand to investigate the antibacterial activity. Ten compounds showed best results regarding the binding mode to the key amino acids in the active site, compared to the ATP ligand. The C-Docker results of the ATP ligand (E=− 142.63 kcal/mol) was used to evaluate the docking interaction of the test compounds as shown

in Fig. 6. Where the main reported binding interactions including Hydrogen Bond Acceptor interaction (HBA) with Ser123, Hydrogen Bond Donor (HBD) interaction with His292, and HBA interaction with Asn296. In addition to HBD with Asp341 and HBA with Lys448 in the central domain was accomplished. While in the C-terminal domain, pi donor hydrogen bond interaction with Ser349 and hydrophobic interaction with Ala352 was noticed. Moreover, charge interactions with Lys125, and Arg327 in the central domain was confirmed [15]. In addition to, 3HBA with Asn344, 1 HBA withThr126, Thr127, Asn150 via the phosphate groups of ATP. And 1 HBD with Gln295 and pi donor hydrogen bond with Thr348.

The docked tested compounds revealed the essential interactions compared to ATP showing comparable competitive behavior with promising predicted antibacterial activity (Fig. 7a, b). Where, 6-(2',3'-Dihydroxy-3-methylbutyl)-8-prenylumbelliferone, scopoline, and 5-methoxymurrayatin were the key discriminators.

While the two bulky compounds named: 8,8''-biskoenigine and murrafoline A, failed to interact within the active site and showed no docking results. Ferulic acid showed the best binding interaction energy (E=− 59.15 kcal/mol), revealing the most stability at the binding pocket. Also, scopolin (E=− 56.92 kcal/mol), 5-methoxymurrayatin (E=− 55.74 kcal/mol), 6-(2',3'-dihydroxy-3-methylbutyl)-8-prenylumbelliferone (E=− 55.44 kcal/mol), sinestin (E=− 50.65 kcal/mol) and sinapine (E=− 47.80 kcal/mol) showed good binding
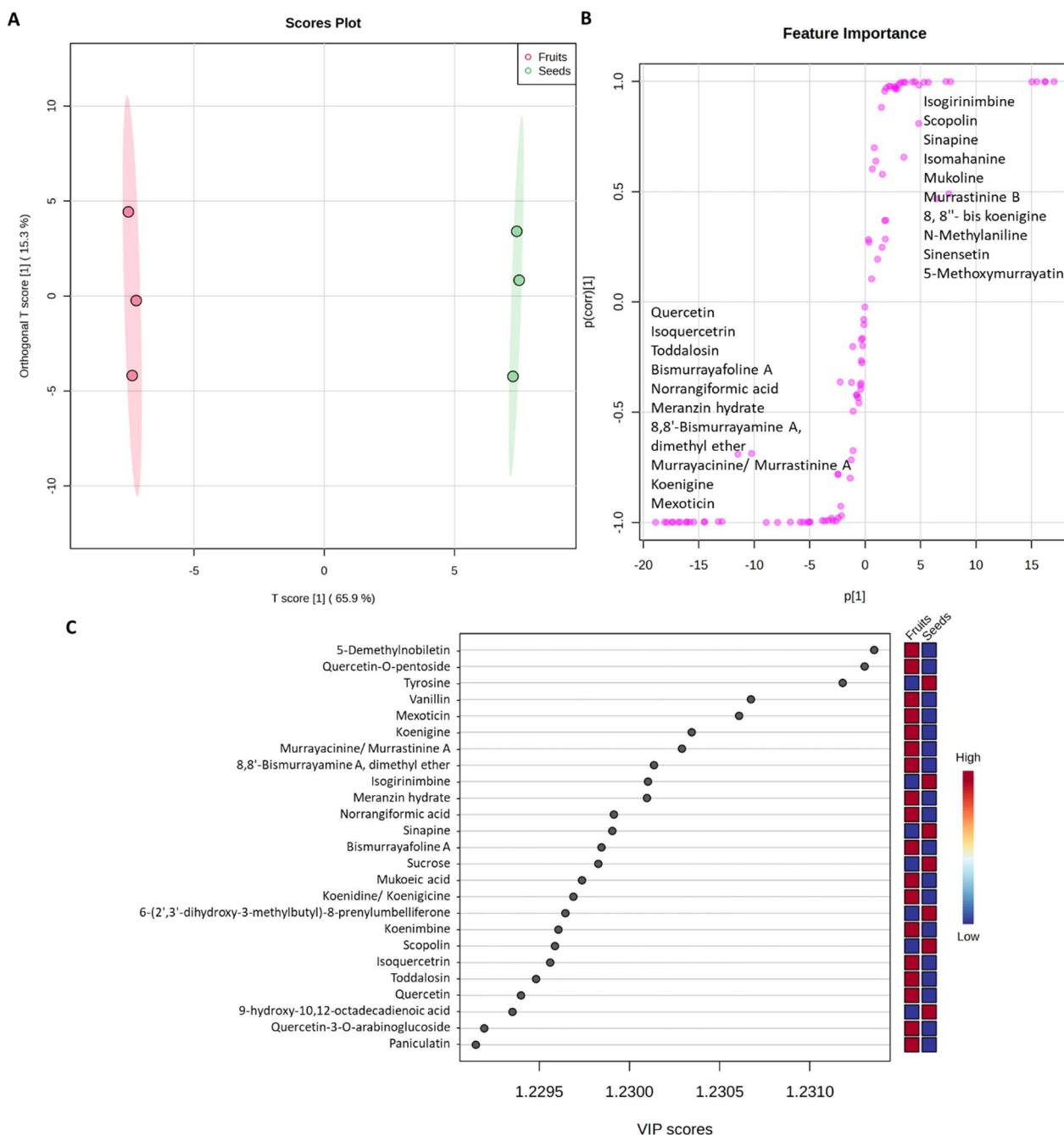
Fig. 5 **A** PLS-DA, **B** S-Plot and **C** VIP Top 25 correlated with the antibacterial activity

interaction energy (Fig. 8a). The visual inspection of the binding mode of the tested compounds confirmed the essential binding interactions with the reported amino acid residues at the active site compared to ATP ligand (Fig. 8b).

Discussion

Murraya koenigii (L.) Sprengel or the Curry plant is a potential medicinal plant, which belongs to the family Rutaceae, highly known for its characteristic aroma and bioactive compounds. Phytochemical analysis of the plant has revealed the presence of proteins, carbohydrates, vitamins, alkaloids, phenolics, and flavonoids providing enormous possibilities to improve consumer

El-Shiekh *et al. Applied Biological Chemistry*   (2024) 67:35

Page 12 of 19

Table 5 Metabolites dominate the active *Murraya koenigii* seeds extract

| Metabolites	Correlation	*p*-value
Antibacterial activity	1	–
Sinapine	0.99912	1.17E−06
Isogirinimbine	0.99835	4.06E−06
6-(2′,3′-dihydroxy-3-methylbutyl)-8-prenylumbelliferone	0.99775	7.58E−06
Scopolin	0.99769	8.00E−06
Sinensetin	0.99666	1.67E−05
8, 8″-bis koenigine	0.9955	3.03E−05
5-Methoxymurrayatin	0.99549	3.05E−05
Mukonine	0.98485	0.000343
Murrastinine B	0.98184	0.000492
Ferulic acid	0.97895	0.00066
Iso-Koenigine	0.97736	0.000763
Mahanimbidine	0.97088	0.001259
Murrafoline A	0.96403	0.001917
Quercitrin	0.95645	0.002804

health and reduce illness risks [11]. Carbazole alkaloids such as koenine, mukoeic acid, mahanimbine, koenimbine, murrayazolidine, murrayazoline, murrayacine and girinimbine have been identified as biologically active compounds with antioxidant, antimicrobial, anti-inflammatory, anthelmintic, antidiarrheal, hepatoprotective, analgesic, and cytotoxic properties [12]. Carbazoles such as mahanimbine, girinimbine, koenimbine, isomahanine

and mahanine were isolated from the pulp of pericarps and seeds of *M. koenigii*. Coumarins were isolated and characterized from the seeds [12, 35, 36], as were a wide range of phospholipids and fatty acids [37]. In our investigation of extracts from the seeds and pericarps of *M. koenigii*, LC/MS/MS analysis allowed the identification and quantification of 40 carbazole alkaloids, 19 coumarins, 11 flavonoids, and five phenolic acids.

Murraya koenigii carbazole alkaloids and coumarins have been demonstrated to be antibacterial, with even greater efficacy than the antibiotics Amikacin and Gentamicin against *Staphylococcus*, *Streptococcus*, *Escherichia coli*, *Pseudomonas*, *Klebsiella*, and *Proteus sp.* [38]. So, the presence of some coumarins such as murrayanone, and scopoline and carbazole alkaloids as mukonine, and iso-koenigine demonstrates the potential of seeds than pericarps as anti *A. baumannii* in our study. Plants of the family Rutaceae are widely used in various parts against Gram-positive and Gram-negative harmful bacterial strains as extracts from this family are dominated by the two important bioactive classes of compounds namely the coumarins and carbazole alkaloids [39, 40]. In-vitro and in-vivo studies revealed promising activity of the seed extracts which were almost as active as the standard Tigecycline. Multidrug-resistant *A. baumannii* is a pathogen that causes severe infections in critically ill people and is infamous for propagating epidemically [41]. By producing pro-inflammatory cytokines, the host activates the innate and adaptive immune systems. However, because over-activation of pro-inflammatory cytokines leads to multi-organ failure, macrophages' early
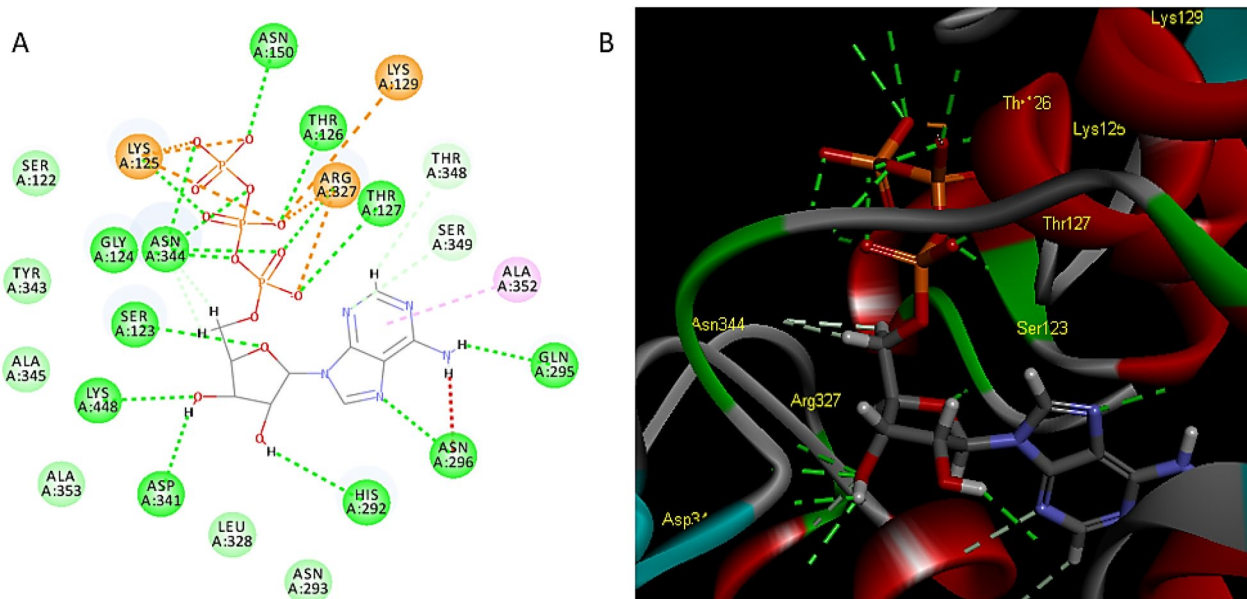
Fig. 6 The C-Docker binding interactions of ATP ligand (E = − 142.63 kcal/mol) after docking on MurF of *Acinetobacter baumannii* (PDB ID: 4QF5) **A** 2D binding interactions, **B** 3D binding interactions
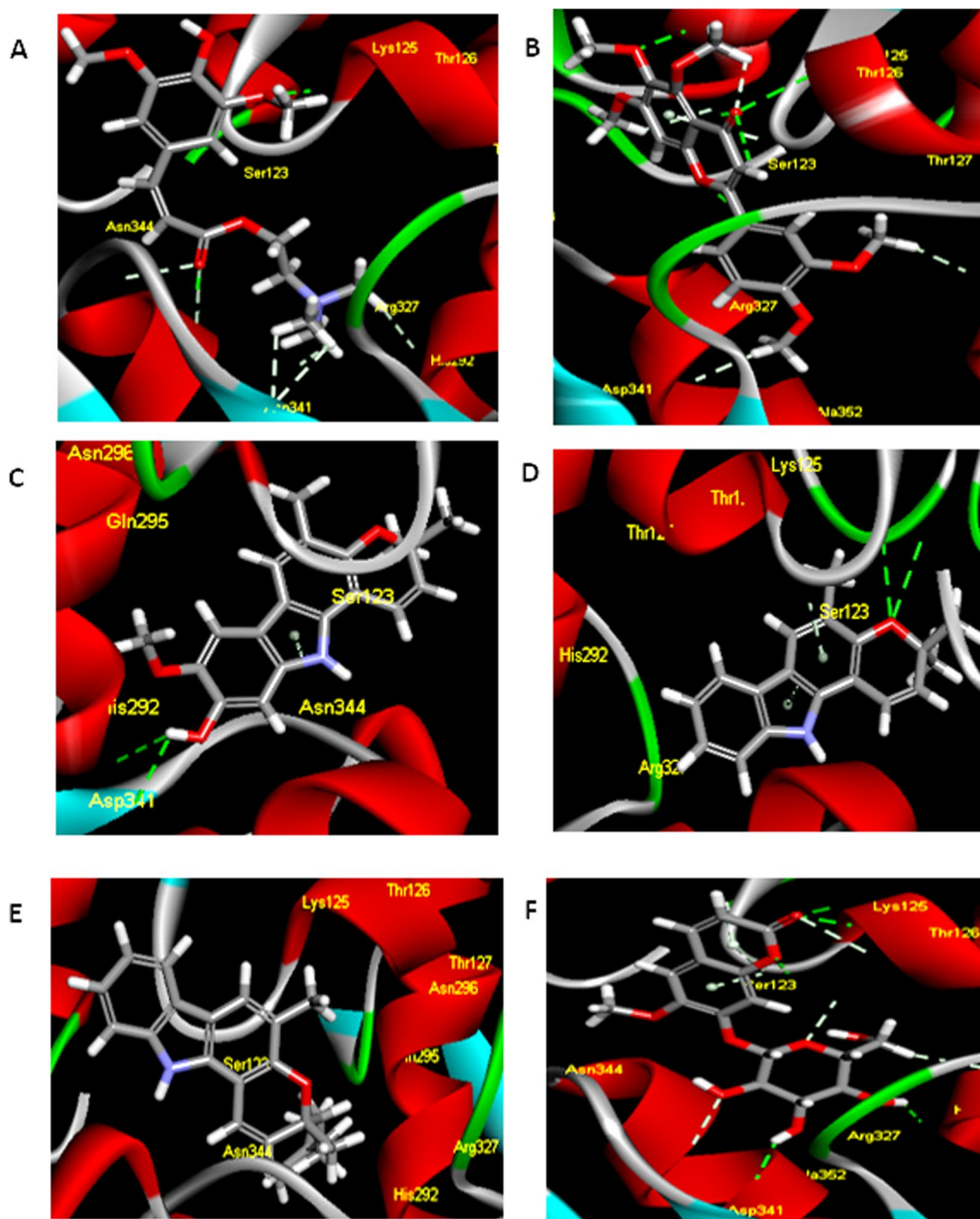
Fig. 7 **a** The 3D binding interactions on MurF of *Acinetobacter baumannii* (PDB ID: 4QF5) of **A** Sinapine (E =-47.80 kcal/mol), **B** Sinestin (E = − 50.65 kcal/mol), **C** Iso-Koenigine (E = − 41.70 kcal/mol), **D** Isogirinimbine (E = − 31.65 kcal/mol), **E** Mahanimbidine (E = − 43.82 kcal/mol) and **F** Scopolin (E = − 56.92 kcal/mol). **b** The 3D binding interactions on MurF of *Acinetobacter baumannii* (PDB ID: 4QF5) of **G** Ferulic acid (E = − 59.15 kcal/mol), **H** Mukonine (E = − 38.45 kcal/mol), **I** 5-Methoxymurrayatin (E = − 55.74 kcal/mol), **J** Quercitrin (E = − 36.41 kcal/mol), **K** Murrastinine B (E = − 39.39 kcal/mol) and **L** 6-(2′,3′-dihydroxy-3-methylbutyl)-8-prenylumbelliferone (E = − 55.44 kcal/mol)

anti-inflammatory action is crucial in fighting infections [42]. Cytokines are key mediators in infections, divided into proinflammatory and anti-inflammatory mediators. We have chosen four proinflammatory mediators, as tumor necrosis factor (TNF)-α, myeloperoxidase (MPO), interleukin (IL)-6, and interferon (IFN)-γ and two anti-inflammatory mediators, including IL-10 and IL-12, to assess the cytokine profile of *A. baumannii*-infected mice and the

protective roles of our treatments [41]. Pro-inflammatory cytokines such as IFN γ, MPO, IL-6, IL-1β, and TNF-α are elevated in *A. baumannii*-infected mice which contributed to apoptosis in the lung tissues [43–45]. In contrast, the anti-inflammatory mediators (IL-10) were decreased in *A. baumannii*-infected mice. Low levels of IL-10, and IL-12 at the first day of *A. baumannii* infection have been attributed to the morbidity and mortality in mice infected
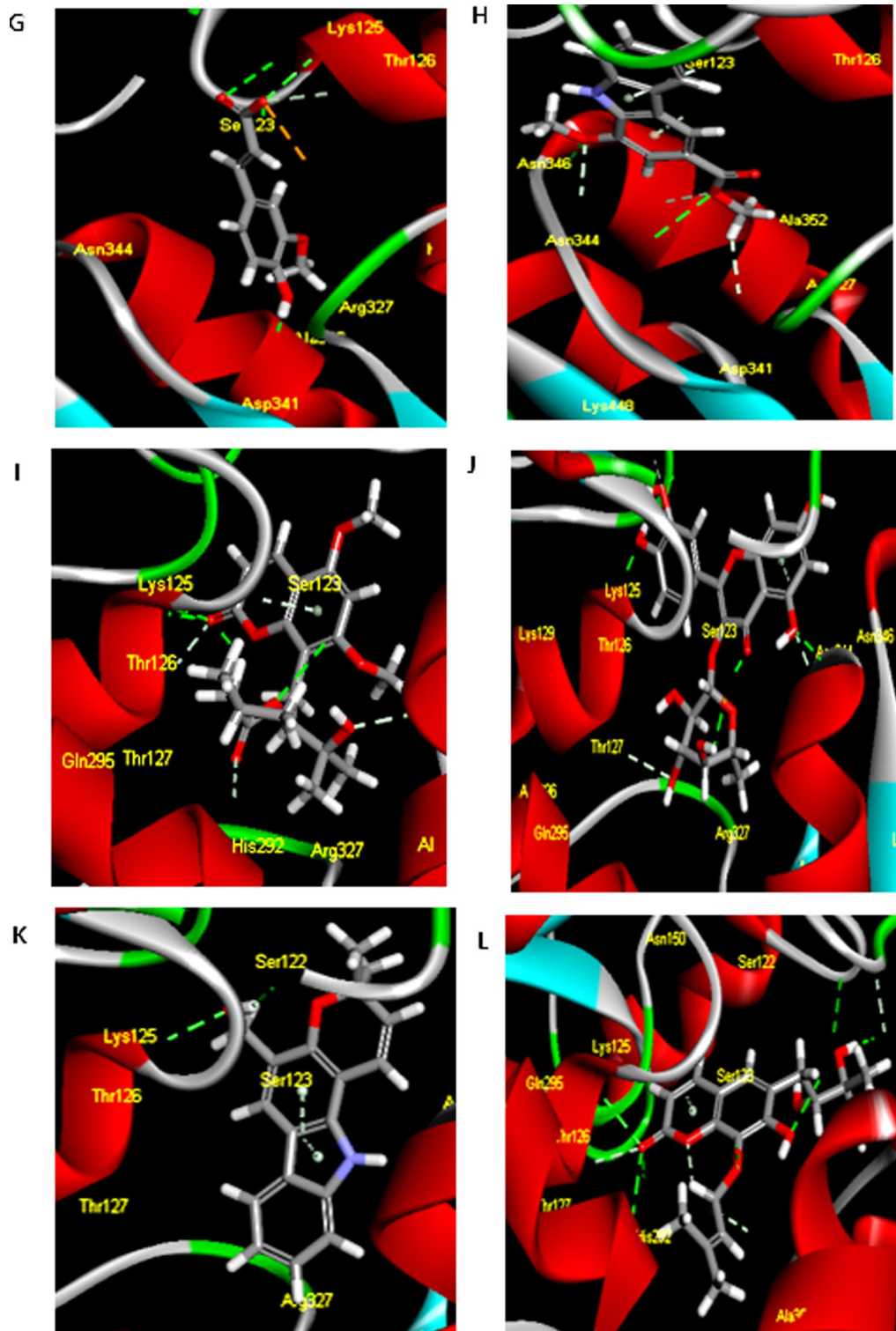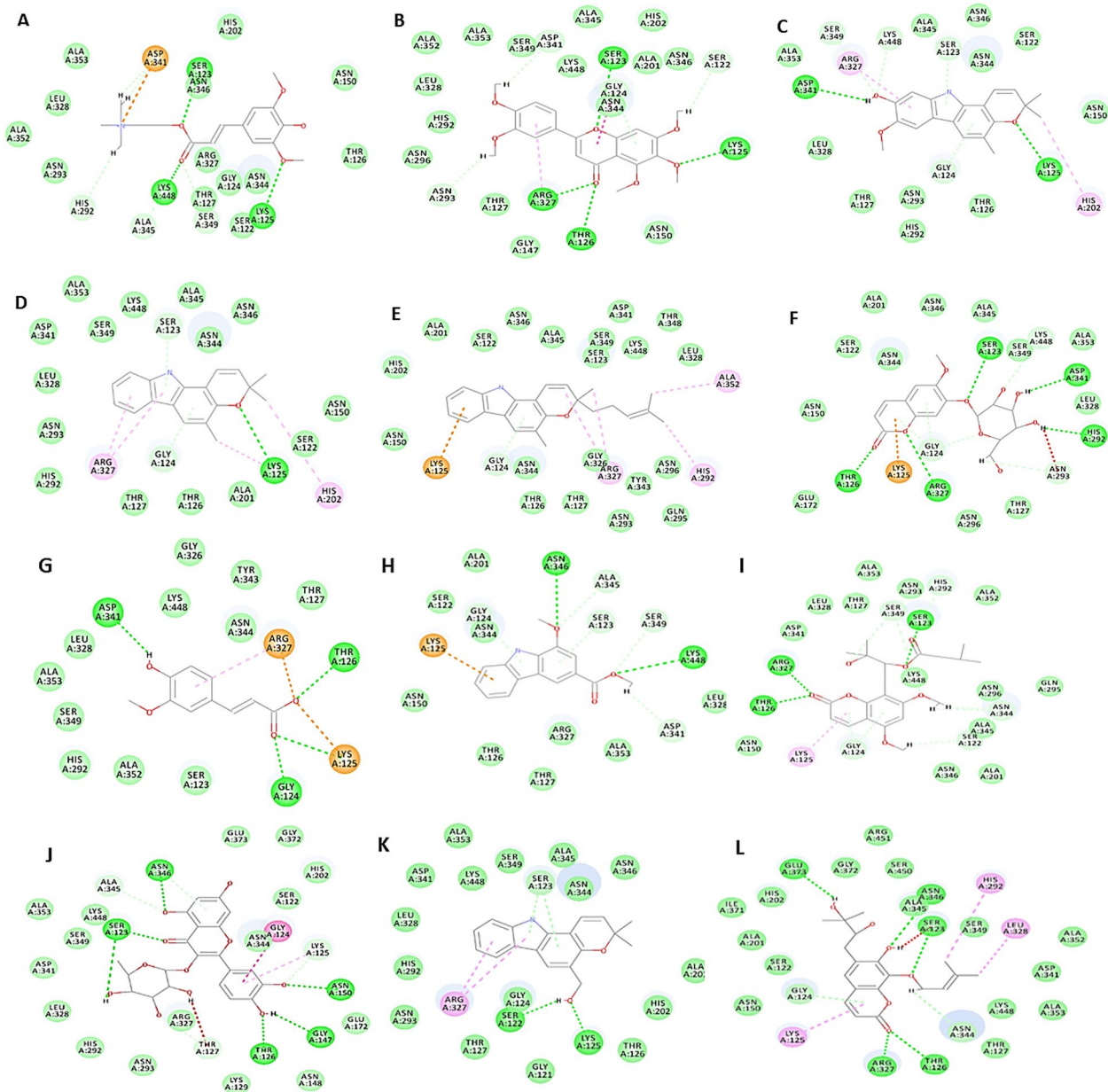
Fig. 7 continued

Fig. 8 **a** The 2D binding mode of **A** Sinapine (E = − 47.80 kcal/mol), **B** Sinestin (E = − 50.65 kcal/mol), **C** Iso-Koenigine (E = − 41.70 kcal/mol), **D** Isogirinimbine (E = − 31.65 kcal/mol), **E** Mahanimbidine (E = − 43.82 kcal/mol) and **F** Scopolin (E = − 56.92 kcal/mol) on with the essential amino acids in the active site of MurF of Acinetobacter baumannii (PDB ID: 4QF5). **b.** The 2D binding mode of **G** ferulic acid (E = − 59.15 kcal/mol), **H** mukonine (E = − 38.45 kcal/mol), **I** 5-methoxymurrayatin (E = − 55.74 kcal/mol), **J** quercitrin (E = − 36.41 kcal/mol), **K** murrastinine B (E = − 39.39 kcal/mol) and **L** 6-(2′,3′-dihydroxy-3-methylbutyl)-8-prenylumbelliferone (E = − 55.44 kcal/mol) on MurF of *Acinetobacter baumannii* (PDB ID: 4QF5)

with *A. baumannii* strains. IL-10 has also been implicated in vaccine-induced protection against *A. baumannii* challenge, where pro-inflammatory cytokines (TNF- and IL-6) levels were significantly reduced and anti-inflammatory cytokine IL-10 levels were significantly increased in lungs and serum, resulting in decreased severity and slow progression of disease [46]. These protective effects were reflected in the hematological parameters measured, and

from the histopathological study also where the treatments alleviated the inflammatory cells infiltration, pulmonary necrosis, and vascular congestion. In addition to the reduction of pulmonary bacterial loads and decreasing the high mortality rates after infection with highly resistant *A. baumannii* strain. The majority of the positively linked biomarker metabolites have been shown to have antibacterial action against distinct strains of bacteria including sinapine

[47], sinensetin [48], quercitrin [49], ferulic acid inhibits tetK and MsrA efflux pumps of multidrug resistance strains [50] in addition to scopolin which is a coumarin derivative that could inhibit the activity of p-glycoprotein (p-gp) and other multidrug resistance proteins [51]. Validation was confirmed by re-docking of the ligand in the target active site showing RMSD value=0.5A° as good validation result. It was reported from the previous literature [52] that the binding mode of ATP at the active site is mainly concerned with the interface between the Central and the C-terminal domains of MurF, showing several interactions with amino acid residues. Where MurF structure is mainly composed of three domains named: the N-terminal, the Central, and the C-terminal domains, respectively [15]. It is known that MurF is essential during the last step in the biosynthesis of monomeric precursor of peptidoglycan within peptidoglycan biosynthesis since it adds (in an ATP-dependent manner) D-Ala-D-Ala dipeptide to UDP-*N*-acetylmuramyl-L-Ala-γ-D-Glu-m-DAP. What makes MurF became an attractive target to develop novel antibiotics. Here, we used computer added drug design (CADD) applying molecular simulation via working on the crystal structure of the Acinetobacter baumannii MurF (AbMurF)-ATP complex [15]. The molecular docking study of the tested compounds revealed twelve promising compounds with comparable and competitive binding mode to ATP as ligand in the binding site. Furthermore, the potential of cabazole alkaloids as antibacterial against multidrug resistant strains was reported several potential actions helping to solve the MDR problems worldwide [19]. Therefore, in order to gain insight to the potential of positively correlated carbazoles including isogirinimbine, 8, 8"- bis koenigine, mukonine, murrastinine B, iso-Koenigine, mahanimbidine, and murrafoline, a further detailed studies of these compounds are required. It is worth highlighting the prophylactic efficacy against *A. baumannii* infection in a murine model of *Murraya koenigii* (L.) Sprengel seeds and pericarps is reported here for the first time.

Trying to deal with the unmanageable multidrug resistance towards the existing antibacterial agents, novel approaches towards the discovery of new targets are required in order to prevent and treat *A. baumannii* infections. While clinical monitoring, developed antibiotics have been successfully targeting enzymes involved in the synthesis of peptidoglycan.

Supplementary Information

The online version contains supplementary material available at https://doi.org/10.1186/s13765-024-00886-7.

Additional file 1: Fig. S1. Tigecycline (TGC 30 µg), amikacin (30 µg), Trimethoprim/sulfamethoxazole (SXT 25µg), cefoxitin (FOX 30µg), Levofloxacin (LVX 5µg), gentamicin (CN 10 µg). **Fig. S2.** *A. baumannii* on LB (Luria-Bertani) agar upon examining pulmonary bacterial loads. **Fig. S3.** Identification of a flavonoid compound (Quercitrin). **Fig. S4.** Identification of a phenolic compound (Chlorogenic acid). **Fig. S5.** Identification of a carbazole alkaloid compound (Murrayacinine). **Fig. S6.** Identification of a carbazole alkaloid compound (Murrayamine A). **Fig. S7.** Inhibition diameter zones obtained by well diffusion method for *A. baumnii* against *M. koenigii* seed extracts and *M. koenigii* fruit extracts. 1. *M. koenigii* seed extracts, 2. *M. koenigii* fruit extracts and 3. DMSO: negative control. **Table S1.** Parameters for MZmine processing of UHPLC-MS/MS data.

Author details
[1]Pharmacognosy Department, Faculty of Pharmacy, Cairo University, Kasr el Aini St., P. B. 11562, Cairo, Egypt. [2]Department of Microbiology and Immunology, Faculty of Pharmacy, Ahram Canadian University, Giza, Egypt. [3]Department of Microbiology and Immunology, Egyptian Drug Authority, Cairo, Egypt. [4]Pharmaceutical Chemistry Department, Faculty of Pharmacy, Future University in Egypt (FUE), Cairo 11835, Egypt. [5]Max Planck Institute of Molecular Plant Physiology, Am Mühlenberg 1, 14476 Potsdam-Golm, Germany. [6]Center for Plant Systems Biology and Biotechnology, Plovdiv 4000, Bulgaria. [7]Department of Pharmacognosy and Natural Products, Faculty of Pharmacy, Menoufia University, Gamal Abd El Nasr St., Shibin Elkom 32511, Menoufia, Egypt. [8]Present Address: The BioActives Lab, Center for Desert Agriculture (CDA), Biological and Environmental Science and Engineering Division (BESE), King Abdullah University of Science and Technology (KAUST), Thuwal 23955-6900, Saudi Arabia.

El-Shiekh *et al. Applied Biological Chemistry*   (2024) 67:35

Page 17 of 19

References

1. Vázquez-López R, Solano-Gálvez SG, Juárez Vignon-Whaley JJ, Abello Vaamonde JA, Padró Alonzo LA, Rivera Reséndiz A et al (2020) *Acinetobacter baumannii* resistance: a real challenge for clinicians. Antibiotics 9:205
2. Ayoub Moubareck C, Hammoudi HD (2020) Insights into *Acinetobacter baumannii*: a review of microbiological, virulence, and resistance traits in a threatening nosocomial pathogen. Antibiotics 9:119
3. Ibrahim S, Al-Saryi N, Al-Kadmy IM, Aziz SN (2021) Multidrug-resistant *Acinetobacter baumannii* as an emerging concern in hospitals. Mol Biol Rep 48:6987–6998
4. Morris FC, Dexter C, Kostoulias X, Uddin MI, Peleg AY (2019) The mechanisms of disease caused by *Acinetobacter baumannii*. Front Microbiol 10:1601
5. Ibrahim ME (2019) Prevalence of *Acinetobacter baumannii* in Saudi Arabia: risk factors, antimicrobial resistance patterns and mechanisms of carbapenem resistance. Ann Clin Microbiol Antimicrob 18:1
6. Qi L, Li H, Zhang C, Liang B, Li J, Wang L et al (2016) Relationship between antibiotic resistance, biofilm formation, and biofilm-specific resistance in *Acinetobacter baumannii*. Front Microbiol 7:483
7. Garnacho-Montero J, Timsit J-F (2019) Managing *Acinetobacter baumannii* infections. Curr Opin Infect Dis 32:69–76
8. Lee C-R, Lee JH, Park M, Park KS, Bae IK, Kim YB et al (2017) Biology of *Acinetobacter baumannii*: pathogenesis, antibiotic resistance mechanisms, and prospective treatment options. Front Cell Infect Microbiol 7:55
9. Sato Y, Ubagai T, Tansho-Nagakawa S, Yoshino Y, Ono Y (2021) Effects of colistin and tigecycline on multidrug-resistant *Acinetobacter baumannii* biofilms: advantages and disadvantages of their combination. Sci Rep 11:11700
10. Arulmoorthy K, Raja K, Sundareswaran S (2019) Physiological and biochemical changes in desiccation sensitive curry leaf (*Murraya koenigii* (L.) Sprengel) seeds. J Phytol 11:38–41
11. Datta HS, Bora D, Purkayastha MD, Choudhury M, Neog M (2023) *Murraya koenigii* (L.) Spreng. Himalayan fruits and berries. Elsevier, Amsterdam, pp 271–287
12. Gahlawat DK, Jakhar S, Dahiya P (2014) *Murraya koenigii* (L.) Spreng: an ethnobotanical, phytochemical and pharmacological review. J Pharmacogn Phytochem 3:109–119
13. Abeysinghe D, Kumara K, Kaushalya K, Chandrika U, Alwis D (2021) Phytochemical screening, total polyphenol, flavonoid content, in vitro antioxidant and antibacterial activities of Sri Lankan varieties of *Murraya koenigii* and *Micromelum minutum* leaves. Heliyon. https://doi.org/10.1016/j.heliyon.2021.e07449
14. Ilangovan SS, Krishna P, Koushika Das SS. A review on anti-microbial properties of Murraya Koenigii. Am J Pharm Res 2016;6.
15. Cha S-S, An YJ, Jeong C-S, Yu JH, Chung KM (2014) ATP-binding mode including a carbamoylated lysine and two Mg2+ ions, and substrate-binding mode in *Acinetobacter baumannii* MurF. Biochem Biophys Res Commun 450:1045–1050
16. El-Shiekh RA, Hassan M, Hashem RA, Abdel-Sattar E (2021) Bioguided isolation of antibiofilm and antibacterial pregnane glycosides from *Caralluma quadrangula*: disarming multidrug-resistant pathogens. Antibiotics 10:811
17. Salem MA, El-Shiekh RA, Hashem RA, Hassan M (2021) In vivo antibacterial activity of star anise (Illicium verum Hook.) Extract Using Murine MRSA skin infection model in relation to its metabolite profile. Infect Drug Resist. https://doi.org/10.2147/IDR.S285940
18. El-Shiekh RA, Elhemely MA, Naguib IA, Bukhari SI, Elshimy R (2023) Luteolin 4′-neohesperidoside inhibits clinically isolated resistant bacteria in vitro and in vivo. Molecules 28:2609
19. Elshimy R, Khawagi WY, Naguib IA, Bukhari SI, El-Shiekh RA (2023) 9-Methoxyellipticine: antibacterial bioactive compound isolated from Ochrosia elliptica Labill. Roots. Metabolites 13:643
20. Ali NB, El-Shiekh RA, Ashour RM, El-Gayed SH, Abdel-Sattar E, Hassan M (2023) In vitro and in vivo antibiofilm activity of red onion scales: an agro-food waste. Molecules 28:355
21. El-Shiekh RA, Elshimy R (2023) Therapeutic effects of Stemmoside C against Salmonella enterica serotype Typhimurium infected BALB/c mice. Steroids 199:109296
22. Salem MA, Jüppner J, Bajdzienko K, Giavalisco P (2016) Protocol: a fast, comprehensive and reproducible one-step extraction method for the rapid preparation of polar and semi-polar metabolites, lipids, proteins, starch and cell wall polymers from a single sample. Plant Methods 12:45
23. Pluskal T, Castillo S, Villar-Briones A, Orešič M (2010) MZmine 2: modular framework for processing, visualizing, and analyzing mass spectrometry-based molecular profile data. BMC Bioinform 11:1–11
24. Nothias L-F, Petras D, Schmid R, Dührkop K, Rainer J, Sarvepalli A et al (2020) Feature-based molecular networking in the GNPS analysis environment. Nat Methods 17:905–908
25. Shannon P, Markiel A, Ozier O, Baliga NS, Wang JT, Ramage D et al (2003) Cytoscape: a software environment for integrated models of biomolecular interaction networks. Genome Res 13:2498–2504
26. Farouk F, El Shimy R, Abdel-Motaleb A, Essam S, Azzazy HM (2020) Detection of *Acinetobacter baumannii* in fresh produce using modified magnetic nanoparticles and PCR. Anal Biochem 609:113890
27. Bauer A (1966) Antibiotic susceptibility testing by a standardized single disc method. Am J Clin Pathol 45:149–158
28. Rana E, Rania AK, Hamdallah Z, Alaa E-DSH, Tarek HE (2018) Study on prevalence and genetic discrimination of methicillin-resistant *Staphylococcus aureus* (MRSA) in Egyptian hospitals. Afr J Microbiol Res 12:629–646
29. Wiegand I, Hilpert K, Hancock RE (2008) Agar and broth dilution methods to determine the minimal inhibitory concentration (MIC) of antimicrobial substances. Nat Protoc 3:163–175
30. Knapp S, de Vos AF, van der Windt GJ, Florquin S, Randle J, van der Poll T (2006) Caspase-1 is an important mediator of lung inflammation during *Acinetobacter baumannii* pneumonia. Inflammatory response to severe bacterial infections 81
31. Harris G, KuoLee R, Xu HH (2017) Chen W (2017) Mouse models of *Acinetobacter baumannii* infection. Curr Protoc Microbiol 46:6G.3.1-6G.3.23
32. Bancroft JD, Gamble M (2008) Theory and practice of histological techniques. Elsevier health sciences
33. Kang M-J, Jang A-R, Park J-Y, Ahn J-H, Lee T-S, Kim D-Y et al (2020) IL-10 protects mice from the lung infection of *Acinetobacter baumannii* and contributes to bacterial clearance by regulating STAT3-mediated MARCO expression in macrophages. Front Immunol 11:270
34. Pang Z, Chong J, Zhou G, de Lima Morais DA, Chang L, Barrette M et al (2021) MetaboAnalyst 5.0: narrowing the gap between raw spectra and functional insights. Nucleic Acids Res 49:W388–W396
35. Adebajo AC, Olugbade TA, Elujoba AA, Aladesanmi AJ, Reisch J (1997) 2", 3"-Epoxyindicolactone from *Murraya koenigii*. Niger J Nat Prod Med 1:21–24
36. Adebajo AC, Reisch J (2000) Minor furocoumarins of *Murraya koenigii*. Fitoterapia 71:334–337
37. Hemavathy J (1991) Lipid composition of *murraya koenigii* seed. J Am Oil Chem Soc 68:651–652
38. Al Harbi H, Irfan UM, Ali S (2016) The antibacterial effect of curry leaves (*Murraya Koenigii*). EJPMR 3:382–387
39. Tamene D, Endale M (2019) Antibacterial activity of coumarins and carbazole alkaloid from roots of clausena anisata. Adv Pharmacol Pharm Sci. https://doi.org/10.1155/2019/5419854
40. Maneerat W, Ritthiwigrom T, Cheenpracha S, Promgool T, Yossathera K, Deachathai S et al (2012) Bioactive carbazole alkaloids from *Clausena wallichii* roots. J Nat Prod 75:741–746
41. de Breij A, Eveillard M, Dijkshoorn L, Van Den Broek PJ, Nibbering PH, Joly-Guillou M-L (2012) Differences in *Acinetobacter baumannii* strains and host innate immune response determine morbidity and mortality in experimental pneumonia. PLoS ONE 7:e30673
42. Lee H, Krishnan M, Kim M, Yoon YK, Kim Y (2022) Rhamnetin, a natural flavonoid, ameliorates organ damage in a mouse model of carbapenem-resistant *Acinetobacter baumannii*-induced sepsis. Int J Mol Sci 23:12895
43. Khan MA, Allemailem KS, Maswadeh H, Younus H (2022) Safety and prophylactic efficacy of liposome-based vaccine against the drug-resistant *Acinetobacter baumannii* in Mice. Pharmaceutics 14:1357
44. Sepahvand S, Madani M, Sepahvand H, Davarpanah MA (2022) Comparative assessment of the mouse immune responses to colistin-resistant and colistin-sensitive isolates of *Acinetobacter baumannii*. Microb Pathog 173:105834

45. Sitarek P, Merecz-Sadowska A, Kowalczyk T, Wieczfinska J, Zajdel R, Śliwiński T (2020) Potential synergistic action of bioactive compounds from plant extracts against skin infecting microorganisms. Int J Mol Sci 21:5105

46. Chen W (2020) Host innate immune responses to *Acinetobacter baumannii* infection. Front Cell Infect Microbiol 10:486

47. Mouterde LM, Peru ALA, Mention MM, Brunissen F, Allais F (2020) Sustainable straightforward synthesis and evaluation of the antioxidant and antimicrobial activity of sinapine and analogues. J Agric Food Chem 68:6998–7004

48. Han Jie L, Jantan I, Yusoff SD, Jalil J, Husain K (2021) Sinensetin: an insight on its pharmacological activities, mechanisms of action and toxicity. Front Pharmacol 11:553404

49. Yassin AS, Abu El Wafa SA, El Menofy NG, Elmerigy AH, Marzouk M (2023) HPLC quantitative analysis of two major flavonoids and antimicrobial effectiveness against multi-drug resistant bacteria of different parts of Khaya senegalensis. Azhar Int J Pharm Med Sci. https://doi.org/10.21608/aijpms.2023.196073.1196

50. Pinheiro PG, Santiago GMP, da Silva FEF, de Araújo ACJ, de Oliveira CRT, Freitas PR et al (2022) Ferulic acid derivatives inhibiting Staphylococcus aureus tetK and MsrA efflux pumps. Biotechnol Rep 34:e00717

51. Lee K, Chae SW, Xia Y, Kim NH, Kim HJ, Rhie S et al (2014) Effect of coumarin derivative-mediated inhibition of P-glycoprotein on oral bioavailability and therapeutic efficacy of paclitaxel. Eur J Pharmacol 723:381–388

52. Ahmad S, Raza S, Uddin R, Azam SS (2017) Binding mode analysis, dynamic simulation and binding free energy calculations of the MurF ligase from *Acinetobacter baumannii*. J Mol Graph Model 77:72–85

53. Mondal P, Natesh J, Penta D, Meeran SM (2022) Extract of *Murraya koenigii* selectively causes genomic instability by altering redox-status via targeting PI3K/AKT/Nrf2/caspase-3 signaling pathway in human non-small cell lung cancer. Phytomedicine 104:154272

54. Thiyam-Holländer U, Aladedunye F, Logan A, Yang H, Diehl BW (2014) Identification and quantification of canolol and related sinapate precursors in Indian mustard oils and Canadian mustard products. Eur J Lipid Sci Technol 116:1664–1674

55. Thiyam U, Claudia P, Jan U, Alfred B (2009) De-oiled rapeseed and a protein isolate: characterization of sinapic acid derivatives by HPLC–DAD and LC–MS. Eur Food Res Technol 229:825–831

56. Singh AP, Wang Y, Olson RM, Luthria D, Banuelos GS, Pasakdee S et al (2017) LC-MS-MS analysis and the antioxidant activity of flavonoids from eggplant skins grown in organic and conventional environments. Food Nutr Sci 8:873

57. Scigelova M, Hornshaw M, Giannakopulos A, Makarov A (2011) Fourier transform mass spectrometry. Mol Cell Proteomics. https://doi.org/10.1074/mcp.O111.009431

58. Barreca D, Gattuso G, Laganà G, Leuzzi U, Bellocco E (2016) C-and O-glycosyl flavonoids in Sanguinello and Tarocco blood orange (*Citrus sinensis* (L.) Osbeck) juice: identification and influence on antioxidant properties and acetylcholinesterase activity. Food Chem 196:619–627

59. Rivera-Pastrana DM, Yahia EM, González-Aguilar GA (2010) Phenolic and carotenoid profiles of papaya fruit (*Carica papaya* L.) and their contents under low temperature storage. J Sci Food Agric 90:2358–2365

60. Aziz S, Sukari M, Rahmani M, Kitajima M, Aimi N, Ahpandi N (2010) Coumarins from *Murraya paniculata* (Rutaceae). Malay J Anal Sci 14:1–5

61. Wang Y, Zang W, Ji S, Cao J, Sun C (2019) Three polymethoxyflavones purified from Ougan (Citrus reticulata Cv. Suavissima) inhibited LPS-induced NO elevation in the neuroglia BV-2 cell line via the JAK2/STAT3 pathway. Nutrients 11:791

62. Wang D, Wang J, Huang X, Tu Y, Ni K (2007) Identification of polymethoxylated flavones from green tangerine peel (Pericarpium Citri Reticulatae Viride) by chromatographic and spectroscopic techniques. J Pharm Biomed Anal 44:63–69

63. Negi N, Abou-Dough AM, Kurosawa M, Kitaji Y, Saito K, Ochi A et al (2015) Coumarins from Murraya exotica collected in Egypt. Nat Prod Commun 10:1934578X1501000420

64. Kinoshita T, Wu J-B, Ho F-C (1996) The isolation of a prenylcoumarin of chemotaxonomic significance from *Murraya paniculata* var. omphalocarpa. Phytochemistry 43:125–128

65. Dai J, Ma D, Fu C, Ma S (2015) Gram scale total synthesis of 2-hydroxy-3-methylcarbazole, Pyrano [3, 2-a] carbazole and prenylcarbazole alkaloids. Eur J Org Chem 2015:5655–5662

66. Wang X, Liang H, Zeng K, Zhao M, Tu P, Li J et al (2019) Panitins AG: coumarin derivatives from *Murraya paniculata* from Guangxi Province, China show variable NO inhibitory activity. Phytochemistry 162:224–231

67. He S-D, Yang X-T, Yan C-C, Jiang Z, Yu S-H, Zhou Y-Y et al (2017) Promising compounds from murraya exotica for cancer metastasis chemoprevention. Integr Cancer Ther 16:556–562

68. Tripathi Y, Anjum N, Rana A (2018) Chemical composition and in vitro antifungal and antioxidant activities of essential oil from *Murraya koenigii* (L.) Spreng. Leaves. Asian J Biomed Pharm Sci 8:6–13

69. Furukawa H, Wu T, Ohta T, Kuoh C (1985) Chemical constituents of *Murraya euchrestifolia* Hayata. Structures of novel carbazolequinones and other new carbazole alkaloids. Chem Pharm Bull 33:4132–4138

70. Rao GV, Rao KS, Annamalai T, Mukhopadhyay T (2009) New coumarin diol from the plant, Chloroxylon swietenia DC. ChemInform. https://doi.org/10.1002/chin.200947189

71. Olennikov DN, Chirikova NK, Kashchenko NI, Nikolaev VM, Kim S-W, Vennos C (2018) Bioactive phenolics of the genus Artemisia (Asteraceae): HPLC-DAD-ESI-TQ-MS/MS profile of the Siberian species and their inhibitory potential against α-amylase and α-glucosidase. Front Pharmacol 9:756

72. Chakraborty D, Bhattacharyya P, Roy S, Bhattacharyya S, Biswas A (1978) Structure and synthesis of mukonine, a new carbazole alkaloid from *Murraya koenigii*. Phytochemistry 17:834–835

73. Liu B-Y, Zhang C, Zeng K-W, Li J, Guo X-Y, Zhao M-B et al (2018) Anti-inflammatory prenylated phenylpropenols and coumarin derivatives from Murraya exotica. J Nat Prod 81:22–33

74. Kinoshita T, Wu J-B, Ho F-C (1996) Prenylcoumarins from Murraya paniculata var omphalocarpa (Rutaceae): the absolute configuration of sibiricin, mexoticin and omphamurin. Chem Pharm Bull 44:1208–1211

75. You C-X, Yang K, Wang C-F, Zhang W-J, Wang Y, Han J et al (2014) Cytotoxic compounds isolated from *Murraya tetramera* Huang. Molecules 19:13225–13234

76. Lv H-N, Zeng K-W, Liu B-Y, Zhang Y, Tu P-F, Jiang Y (2015) Biological activity and chemical constituents of essential oil and extracts of *Murraya microphylla*. Nat Prod Commun 10:1934578X1501000935

77. Wu T-S (1988) Coumarins from the leaves of *Murraya paniculata*. Phytochemistry 27:2357–2358

78. Furukawa H, Wu T, Kuoh C (1985) Structures of murrafoline-B and-C, new binary carbazole alkaloids from *Murraya euchrestifolia*. Chem Pharm Bull 33:2611–2613

79. Ito C, Furukawa H (1987) Constituents of Murraya exotica L. structure elucidation of new coumarins. Chem Pharm Bull 35:4277–4285

80. Wang Y-S, He H-P, Shen Y-M, Hong X, Hao X-J (2003) Two new carbazole alkaloids from Murraya k Oenigii. J Nat Prod 66:416–418

81. Yang H, Zhou Q, Peng C, Liu L, Xie X, Xiong L et al (2014) Coumarins from Leonurus japonicus and their anti-platelet aggregative activity. Zhongguo Zhong yao za zhi = Zhongguo Zhongyao Zazhi= China J Chin Mater Med 39:4356–4359

82. Kureel S, Kapil R, Popli S (1969) Terpenoid alkaloids from *Murraya koenigii* spreng.-II.: the constitution of cyclomahanimbine, bicyclomahanimbine, and mahanimbidine. Tetrahedron Lett 10:3857–3862

83. Murray RD, Zeghdi S (1989) Synthesis of the natural coumarins, murraol (CM-c2), trans-dehydroosthol and swietenocoumarin G. Phytochemistry 28:227–230

84. Ochung' AA, Manguro LAO, Owuor PO, Jondiko IO, Nyunja RA, Akala H et al (2015) Bioactive carbazole alkaloids from *Alysicarpus ovalifolius* (Schumach). J Korean Soc Appl Biol Chem 58:839–846

85. Schuster C, Börger C, Julich-Gruner KK, Hesse R, Jäger A, Kaufmann G et al (2014) Synthesis of 2-hydroxy-7-methylcarbazole, glycozolicine, mukoline, mukolidine, sansoakamine, clausine-H, and clausine-K and structural revision of clausine-TY. Eur J Org Chem 2014:4741–4752

86. Furukawa H, Wu T, Ohta T (1983) Bismurrayafoline-A and-B, Two Novel" Dimeric" Carbazole Alkaloids from Murraya euchrestifolia. Chem Pharm Bull 31:4202–4205

87. Tan S-P, Ali AM, Nafiah MA, Awang K, Ahmad K (2015) Isolation and cytotoxic investigation of new carbazole alkaloids from *Murraya koenigii* (Linn.) Spreng. Tetrahedron 71:3946–3953

88. Joshi B, Kamat V, Gawad D (1970) On the structures of girinimbine, mahanimbine, isomahanimbine, koenimbidine and murrayacine. Tetrahedron 26:1475–1482

89. Hesse R, Gruner KK, Kataeva O, Schmidt AW, Knölker HJ (2013) Efficient construction of Pyrano [3, 2-a] carbazoles: application to a biomimetic total synthesis of cyclized monoterpenoid Pyrano [3, 2-a] carbazole alkaloids. Chem A Eur J 19:14098–14111

90. McPhail AT, Wu T-S, Ohta T, Furukawa H (1983) Structure of (±)-murrafoline, a novel biscarbazole alkaloid from *Murraya euchrestifolia*. Tetrahedron Lett 24:5377–5380

91. Wu T-S (1991) Murrayamine-A,-B,-C and (+)-mahanine, carbazole alkaloids from *Murraya euchrestifolia*. Phytochemistry 30:1048–1051

92. Ito C, Thoyama Y, Omura M, Kajiura I, Furukawa H (1993) Alkaloidal constituents of *Murraya koenigii*. Isolation and structural elucidation of novel binary carbazolequinones and carbazole alkaloids. Chem Pharm Bull 41:2096–2100

93. Reisch J, Aladesanmi AJ (1994) Two carbazole alkaloids from Murraya koenigii. Phytochemistry 36(4):1073–1076. https://doi.org/10.1016/S0031-9422(00)90494-1

94. Chakrabarty M, Nath AC, Khasnobis S, Chakrabarty M, Konda Y, Harigaya Y et al (1997) Carbazole alkaloids from *Murraya koenigii*. Phytochemistry 46:751–755

95. Steck W (1972) Paniculatin, a new coumarin from *Murraya paniculata* (L.) Jack. Can J Chem 50:443–445

96. Ashokkumar K, Selvaraj K, Km SD (2013) Reverse phase-high performance liquid chromatography-diode array detector (RP-HPLC-DAD) analysis of flavonoids profile from curry leaf (*Murraya koenigii* L.). J Med Plants Res 7:3393–3399

97. Fiebig M, Pezzuto JM, Soejarto DD, Kinghorn AD (1985) Koenoline, a further cytotoxic carbazole alkaloid from *Murraya koenigii*. Phytochemistry 24:3041–3043

98. Bernal P, Tamariz J (2007) Total synthesis of murrayanine involving 4, 5-dimethyleneoxazolidin-2-ones and a palladium (0)-catalyzed diaryl insertion. Helv Chim Acta 90:1449–1454

99. Ruangrungsi N, Ariyaprayoon J, Lange GL, Organ MG (1990) Three new carbazole alkaloids isolated from *Murraya siamensis*. J Nat Prod 53:946–952

100. Chakraborty D (1993) Chemistry and biology of carbazole alkaloids. Alkaloids Chem Pharmacol 44:257–364

101. Avila-Melo JL, Benavides A, Fuentes-Gutiérrez A, Tamariz J, Jiménez-Vázquez HA (2021) Total synthesis of the natural carbazoles O-demethylmurrayanine and Murrastanine A, and of a C4, C4′ symmetric murrastanine A dimer from N-phenyl-4, 5-dimethylene-1, 3-oxazolidin-2-one. Synthesis 53:2201–2211

Publisher's Note